2026, Scienceline Publication
World's Veterinary Journal
World Vet J, 16(2): 560-572.
ISSN 2322-4568

DOI: https://dx.doi.org/10.54203/scil.2026.wvj53
PII: S232245682600053-16

Fabrication and Evaluation of Absorbable Sutures Derived from Cellulose Fibers of Pineapple (*Ananas comosus*) Leaves

Chau Buu Tran[1], Chau Thuy Ngoc Nguyen[1], Khiem Gia Mai[2], Thuy Thanh Nguyen[1], and Thuong Thi Nguyen[1]*

[1] *Faculty of Animal Science and Veterinary Medicine, Nong Lam University, Ho Chi Minh City, 71308, Vietnam*
[2] *Faculty of Agronomy, Nong Lam University, Ho Chi Minh City, 71308, Vietnam*

*Corresponding author's Email: thuong.nguyenthi@hcmuaf.edu.vn

ORIGINAL ARTICLE
Received: April 03, 2026
Revised: May 06, 2026
Accepted: June 07, 2026
Published: June 30, 2026

ABSTRACT

Developing sustainable and biodegradable veterinary biomaterials is crucial for addressing limitations of synthetic sutures and avoiding secondary suture removal. The present study aimed to develop a novel, eco-friendly suture derived from pineapple leaves as an alternative to synthetic surgical threads and to assess its functional and clinical potential. The present study fabricated absorbable veterinary sutures from pineapple leaf fibers (PALF) via alkaline treatment and 2,2,6,6-tetramethylpiperidine-1-oxyl (TEMPO)-mediated oxidation. The purified fibers, characterized by an average diameter of 53.61 ± 1.89 µm were successfully isolated via alkaline treatment and TEMPO-mediated oxidation, dyed naturally with *Peristrophe bivalvis*, coated with 1% chitosan, and subsequently twisted into size 3/0 sutures. *In vitro* degradation in phosphate buffer solution over four weeks confirmed their biodegradability, as demonstrated by increased fragility and strand separation. For the *in vivo* trial, 24 male mice (20-24 grams) were housed at a density of three mice per cage throughout the cultivation periods of 7, 14, 28, and 45 days. The mice were divided into two groups, including those that underwent surgery and were treated with PALF sutures (experimental group) and those that were treated with Polyglactin 910 (control group). A 2-3 cm dorsal-to-abdominal skin incision was made to expose the subcutaneous tissue, followed by a 1-2 cm connective tissue incision to establish the wound model for testing PALF sutures. Specific parameters, including the degree of edema and erythema, localized temperature, and the presence of exudate, suppuration, secondary infection, and hemorrhage, were assessed for each group. Critical complications, including wound dehiscence or marginal necrosis, were recorded. The current results demonstrated that PALF sutures were biocompatible and followed a healing pathway similar to that of Polyglactin 910. The present results revealed that PALF sutures had significantly lower secondary infection scores (0.08 ± 0.28) than Polyglactin 910 (0.58 ± 0.90), indicating superior anti-infective property. All clinical inflammatory signs completely resolved by day 45. The TEMPO-oxidized PALF sutures were a viable, biocompatible, and sustainable alternative to absorbable veterinary sutures, demonstrating effective tissue healing and a significantly lower incidence of secondary infection.

Keywords: Absorbable suture, *Ananas comosus*, Cellulose, Pineapple leaf, Mice

INTRODUCTION

Recent studies on bio-based materials have highlighted their safety and eco-friendly characteristics (Jain and Sinhan, 2022). Pineapple leaf fiber (PALF) is a natural fiber that can be processed to achieve a high cellulose content (Abu et al., 2019). The PALF cellulose has hydroxyl (-OH) groups that form stable polymer networks (Yadav et al., 2025). As a result of these polymer networks, cellulose fibers were macerated and developed into a productive technology, which was applied to composite materials across many fields, such as textiles, paper, and reinforced plastics (Mayakannan et al., 2023). A wide range of physicochemical and biotechnological approaches, such as alkaline treatment and hydrothermal pretreatment at high pressure, have been developed to accurately extract and isolate the components of fiber matrices, thereby optimizing the use of pineapple leaf waste in high-value applications (Saini et al., 2022; Esquivel et al., 2025; Liao et al., 2025). In Vietnam, the total area of pineapple cultivation encompasses approximately 52,000 hectares, of which 48,000 hectares are harvested annually (Pham et al., 2024). This large-scale production generated substantial agricultural by-products. Kien Giang, one of the Mekong Delta's major provinces in Vietnam, has about 7,850 hectares and an annual production of over 115,000 tons (Pham et al., 2024). Traditionally, post-harvest pineapple foliage has been regarded as a low-value residue, typically either left in the field or incorporated into the soil as green manure (Saini et al., 2023; Lalhruaitluangi and Mandal, 2024). Moreover, in fruit and vegetable processing facilities, most pineapple by-products are discarded in landfills, thereby imposing a significant environmental burden. A previous

To cite this paper: Tran CB, Nguyen CTN, Mai KG, Nguyen TT, and Nguyen TT (2026). Fabrication and Evaluation of Absorbable Sutures Derived from Cellulose Fibers of Pineapple (*Ananas comosus*) Leaves. *World Vet. J.*, 16(2): 560-572. DOI: https://dx.doi.org/10.54203/scil.2026.wvj53

study has indicated that PALF was applied in the processing of high-value products, including textile-grade fibers, fiber-reinforced composites, and bromelain enzymes (Hazarika et al., 2018).

In surgery, absorbable sutures play a pivotal role in securing tissues, supporting the wound-healing cascade, and facilitating suture removal post-operation (Nappi, 2025). There are currently natural absorbable sutures, such as catgut and collagen (Gupta, 2025); neither is an ideal suture material for clinical use. Catgut suture and collagen sutures demonstrated unpredictable degradation during inflammation and suboptimal mechanical performance, including hydration-induced swelling and unreliable knot security (Pillai and Sharma, 2010). Besides natural absorbable sutures, polyglactin 910 is a synthetic absorbable suture composed of a 9:1 copolymer ratio of glycolide and lactide (Öksüz, 2024). Using Polyglactin 910 for suturing subcutaneous tissue after cesarean section is an effective solution to prevent complications such as fluid accumulation or wound infection. With clinical similarities to Polyglycolic acid, Polyglactin 910 has demonstrated its role as a reliable suture material, supporting patients' return to normal activities within a similar timeframe (Devi et al, 2023). Consequently, there is strong potential to develop bio-based absorbable sutures derived from natural sources and environmentally sustainable. Cellulose extracted from PALF is considered a highly promising material due to its superior mechanical strength, which optimizes biocompatibility and degradation profiles (Asim et al., 2015). Additionally, PALF benefits from the plentiful supply of raw materials derived from agricultural by-products. Therefore, the present study aimed to develop sustainable absorbable veterinary sutures from PALF via alkaline extraction and 2,2,6,6-tetramethylpiperidine-1-oxyl (TEMPO)-mediated oxidation, and subsequently validate their mechanical performance, *in vitro* biodegradation kinetics, and *in vivo* tissue-healing efficiency in mice.

MATERIALS AND METHODS

Ethical approval

The study employed an incisional wound model, including wound closure, postoperative monitoring, clinical evaluation, and post-mortem analysis, in accordance with the guidelines of the Animal Welfare Council at Nong Lam University, Ho Chi Minh City, Vietnam. The authors considered ethical concerns, consent, animal welfare, and safety procedures before conducting the study.

Materials

A total of 3 kg of fresh pineapple leaves (*Ananas comosus* var. Queen) were collected after fruit harvesting from a pineapple farm in An Giang Province, Vietnam, during the harvest season (July to August, 2025). A total of 200 g of fresh leaves of *Peristrophe bivalvis*, locally known as Magenta, harvested from the same farm in An Giang Province, was used as a natural colorant for the chromogenic functionalization of cellulose filaments (Evitasari et al., 2019).

The materials used in the present study included TEMPO (Cool Chemical Science and Technology Company, China) chitosan (Biobasic Company, Canada), sodium bromide (NaBr; Xilong Scientific Company, China) , sodium hypochlorite (NaClO; Xilong Scientific Company, China), hydrochloric acid (HCl; Xilong Scientific Company, China), acetic acid (CH_3COOH; Xilong Scientific Company, China), ethanol (Xilong Scientific Company, China), phosphate-buttered saline 10X solution (PBS; pH 7.2-7.6; Fisher Scientific Company, USA), and Sodium hydroxide (NaOH; Guangdong Guanghua Sci-Tech Company, China). Experimental equipment included a Cobalt-60 gamma irradiator, a Fourier transform infrared (FTIR) spectrometer (FTIR-6X1 type A, Serial No. A004962116, Jasco, Japan), and a field-emission scanning electron microscope (FE-SEM; S-4800, Hitachi, Japan). The tensile properties of PLAF single-strand suture samples were evaluated using a manual dead-weight loading configuration adapted from the ASTM D2256/D2256M protocols (ASTM, 2002).

Pineapple leaf fiber-derived suture fabrication

Decortication of pineapple leaf cellulose fibers

A total of 3 kg of pineapple leaves were mechanically decorticated by manually scraping the surface using a metal spoon to remove the outer waxy epidermis and parenchyma tissues. This process exposed the longitudinal vascular bundles of cellulose fibers. The decortication process yielded approximately 45 g of fiber bundles, which were then thoroughly rinsed with distilled water to remove any remaining impurities.

Alkaline treatment of pineapple leaf fibers

Alkaline treatment was performed by immersing the cellulose fibers in a 3% (w/v) NaOH solution at room temperature (22°C) for 60 minutes, maintaining a liquor ratio of 1:20. This process aimed to disrupt the hydrogen bonding in the cellulose fiber's network structure, adapted from Motaleb et al. (2018), and solubilize non-cellulosic components, such as lignin and hemicellulose. Consequently, alkaline treatment yielded higher-purity cellulose fiber, defibrillated clustered bundles, and increased surface roughness, thereby enhancing interfacial adhesion (Gnanasekaran

et al., 2021), potentially increasing inter-fiber friction during the braiding process. Finally, all 45 g of treated fibers were thoroughly rinsed with distilled water to remove residual NaOH, then air-dried at room temperature (22°C) for 15 minutes.

TEMPO-mediated oxidation of pineapple leaf fiber

The TEMPO-mediated oxidation of the PALF cellulose fibers was conducted in the TORC system (TEMPO/NaBr/NaClO; Araya-Chavarría et al., 2022). The TEMPO/NaBr catalyst mixture was prepared with a molar ratio of 1:10 mmol/g of fiber and dissolved in an appropriate volume of distilled water until the fibers' viscosity disappeared. After the alkaline treatment, the fibers were added to the TEMPO/NaBr solution and stirred continuously to ensure the fibers were fully wetted (Araya-Chavarría et al., 2022). Before initiating the oxidation reaction, the pH was adjusted to 10-11 with 0.5 M NaOH to optimize the selective oxidation of cellulose (Lin et al., 2018). Once the target pH was reached, NaClO at a concentration of 5 mmol/g of fiber was added to the solution by slow, dropwise addition. The mixture was stirred continuously for 45-60 minutes to control the oxidation rate and maintain pH stability. During the reaction, 0.5 M NaOH was added as required to maintain a pH of 10-11, which was continuously monitored with litmus paper. After the addition of NaClO, the mixture was continuously stirred for 10-15 minutes to ensure complete oxidation. Subsequently, the reaction was stopped by adding a 2:1 ethanol-NaClO mixture, and the mixture was stirred for 2-5 minutes to neutralize residual NaClO and stabilize the oxidized product. Finally, the mixture was neutralized to pH 7.0 by dropwise addition of 0.1 M HCl. The PALF cellulose fibers were then thoroughly rinsed with distilled water and air-dried at room temperature for 15 minutes.

Natural dyeing process of pineapple leaf fiber

The natural dyeing process of the PALF-derived cellulose fibers was conducted using an anthocyanin-rich extract from magenta leaves (Le et al., 2021). The dye was prepared by aqueous extraction, in which dried leaves were immersed in distilled water at a 1:10 (w/v) material-to-solvent ratio. The mixture was heated at 80-90°C for 10-15 minutes, then filtered through Whatman No. 1 filter paper (Merck Company, Germany) with a pore size of 11 µm to obtain a clear pigment solution. The dye bath pH was adjusted to 3-4 using acetic acid (CH3COOH) to stabilize the anthocyanins and preserve their purple hue. The cellulose fibers were then immersed in the dye solution at 60-70°C for 30-60 minutes to enhance dye adsorption. After dyeing, the fibers were gently rinsed with cold distilled water and air-dried at room temperature. This procedure was based on findings that anthocyanins were most stable in acidic media and are effective as natural colorants for cellulosic substrates (Le et al., 2021).

Suture fabrication and chitosan coating of pineapple leaf fiber

The TEMPO-oxidized cellulose monofilaments were twisted (2-3 strands) to achieve a 3/0 suture size. Subsequently, a 1% (w/v) chitosan solution, characterized by a molecular weight of 10-20 kDa and a degree of deacetylation of at least 90%, was prepared by dispersing 1g of chitosan in 100 mL of 1% acetic acid buffer. The mixture was stirred at 400 rpm for six hours to ensure homogeneity (Akter et al., 2020). The twisted filaments were immersed in the chitosan solution at a 1:20 (w/v) ratio for 60 minutes at room temperature to ensure a uniform polymeric layer. Following a brief rinse with distilled water, a secondary coating was applied for another 60 minutes. After the coating process, the fibers were rinsed three times with distilled water to remove excess surface chitosan and dried in a laboratory drying oven (UF55, Memmert, Germany) at 40°C for 60 minutes.

Gamma irradiation sterilization of pineapple leaf fiber sutures

The radiation processing of the developed PALF sutures was performed at the Biotechnology Center of Ho Chi Minh City, Inc., Vietnam, using a Co-60 gamma source at a dose rate of 5 kGy/h for four hours, yielding a total dose of 20 kGy. The baseline understanding of radiation-induced chemical effects, including macromolecular chain scission and free-radical mechanisms in polymer backbones, was derived from studies on gamma-irradiated polylactic acid (PLA) and PLA/cellulose fibers (Aouat et al., 2019), along with established biopolymer radiation standards (Al-Assaf et al., 2016).

Evaluation of breaking force

The tensile properties of the single-strand suture samples were evaluated using a manual dead-weight loading configuration, adapted from ASTM D2256/D2256M protocols (ASTM, 2002). One end of the thread was secured to a fixed point with a type O knot to establish the initial gauge length (cm), while the opposing end was progressively loaded with calibrated metal weights until complete rupture occurred. The time-to-break (seconds) was recorded to ensure consistency.

The characteristics of pineapple leaf fiber sutures

Morphology and structure of pineapple leaf fiber sutures

An FTIR equipped with an ATR PRO ONE X tool (S/N: A002962140, JASCO, Japan) was employed to assess the analysis of fiber chemical composition. This analysis aimed to examine the chemical functional composition of the fibers

before and after chemical treatment in the wavenumber range of 4,000-400 cm^{-1} (Dharanendra et al., 2025). Observation of surface morphology and fiber dimensions was carried out using the FE-SEM to observe the surface morphology of the fibers post-chemical treatment. The SEM micrographs were subsequently processed in ImageJ version 1.53 to calculate fiber diameters (Götz et al., 2021).

In vitro degradation of pineapple leaf fiber sutures

The sutures were immersed in 50 mL of PBS with a pH range of 7.2 to 7.6 during the two- and four-week periods. The degradation level of the sutures was subsequently analyzed using FTIR spectroscopy (4,000- 400 cm^{-1}) at the Ho Chi Minh City Biotechnology Center, Vietnam, following the methodology described by Antoniac et al. (2021).

***In vivo* evaluation and tissue compatibility of pineapple leaf fiber sutures**

Experimental design

A one-factor randomized complete block design was employed, which consisted of two suture types, including the bio-based PALF sutures 3/0 and the commercial Polyglactin 910 3/0 (Medico, China) as the control. The clinical performance of tissues was assessed based on five key inflammatory parameters, including edema, erythema, exudate formation, secondary infection, and hemorrhage, which were evaluated at 7, 14, 28, and 45 postoperative days, using a semi-quantitative scoring system and a clinical scoring system for evaluating local tissue reactions to sutures in mice (Karner et al., 2020). These time points were strategically selected to encompass the entire wound-healing process, from the acute and subacute inflammatory phases to complete tissue regeneration. Scores ranged from 0 to 3, corresponding to absent, mild, moderate, and severe reactions, respectively, adopted from the study of Karner et al. (2020; Table 1). Following a completely randomized design (CRD), mice were divided into two treatment groups, with three independent biological replicates per group at each time point.

Table 1. Clinical evaluation scale for in *vivo* suture response in mice

Score	Edema	Erythema	Exudate formation	Secondary infection	Hemorrhage
0	None	None	None	None	None
1	Mild swelling	Pale pink	Serous fluid	Localized infection	Mild peri-sutural redness
2	Moderate swelling	Distinct redness	Slightly cloudy discharge	Extension to adjacent tissues	Slight oozing of blood
3	Severe swelling, suture site deformation	Deep red, extensive spreading	Purulent discharge (pus)	Systemic involvement	Active bleeding

Scores: 0: None, 1: Mild, 2: Moderate, 3: Severe. Source of scoring adopted from the study of Karner et al. (2020)

Animals

A total of 24 healthy adult male albino mice, each 2 months old and weighing between 20 and 24 g, were randomly assigned to two groups (n = 12 per group, with three replicates) corresponding to two suture types (Karner et al., 2020). One group was treated exclusively with PALF sutures (experimental group), and the other group was treated with Polyglactin 910 (control group).

The experimental setup was specifically designed to eliminate immune interference by separating groups, ensuring that inflammatory or healing responses were solely due to the suture material and preventing cross-interaction or signal interference. Only male mice were used in the present experiment to minimize biological variability associated with hormonal fluctuations. Female mice undergo estrous cycles, during which estrogen and progesterone levels vary and can significantly influence inflammatory responses and tissue repair processes (Beery et al., 2011). These hormonal variations may introduce additional variability in wound healing outcomes. Therefore, using male mice ensured more stable physiological conditions and improved the reliability of the experimental results. Three mice were euthanized at each time point (at 7, 14, 28, and 45 days) to collect tissue samples. The sample size was determined in accordance with ethical considerations to minimize animal use, while ensuring an adequate number of biological replicates for histological and inflammatory evaluations, in alignment with the principles of the Replacement, reduction, and refinement (3Rs) in animal studies (Kilkenny et al., 2010; MacArthur, 2018). This design ensured independent measurements and avoided repeated sampling bias.

Housing and feeding

Prior to the surgical procedure, the mice underwent a 7-day acclimatization period under controlled environmental conditions to ensure physiological and psychological stability (Obernier et al., 2006). The mice were housed in eight iron cages (three mice per cage, grouped by treatment and designated evaluation time point) measuring 47 × 30 × 30 cm, with rice husk used as bedding material. The rice husk bedding was completely replaced every 2-3 days or spot-cleaned earlier when excessive feces or urine accumulated. Established protocols for nutrition and hygiene were strictly maintained to ensure uniformity across all mice, eliminating potential confounding variables that could interfere with the experimental outcomes. The feed, manufactured by Vienovo in Vietnam, comprised pellets containing 17% crude protein, 1.5% calcium, and 2,700 kcal of energy, in accordance with the National Research Council (NRC, 2011).

Anesthesia and surgical procedure

Pre-operative preparations were carefully performed for all surgical procedures. Before surgery, the mice's health status, including normal dietary intake, active locomotion, and the absence of aggressive behavior or fighting, was thoroughly re-evaluated to ensure the absence of any pathologies. To reduce handling-related stress, the daily welfare of animals was evaluated using four key visual clinical indicators, including activity level, respiratory health, coat condition, and body posture (University of Queensland, 2021). Following a general health assessment, general anesthesia was induced using a combination of tiletamine 25 mg/mL and zolazepam 25 mg/mL (Zoletil 50, Virbac Company, Vietnam) at 1 mg/kg (Cagle et al., 2017). When the mice achieved a deep state of anesthesia, the dorsal-lateral region was shaved and disinfected with alcohol and Povidone-iodine 10%. A 2-3 cm skin incision was made from the dorsal midline towards the abdominal area. This incision was carefully performed to an appropriate depth to expose the subcutaneous connective tissue, followed by a 1-2 cm incision through the underlying connective tissue layer to establish the wound model (Kandimalla et al., 2016). In the experimental group, the subcutaneous incisions were closed using PALF 3/0 sutures. For the control group, the same layer (the underlying connective tissue) was sutured with 3/0 Polyglactin 910. The skin layer was closed with 3/0 nylon (Medico, China). All wounds were sealed with a simple interrupted pattern; this method provided strong security for each strand but increased the volume of foreign bodies at the wound site due to multiple knots, thereby increasing closure times (Nair et al., 2023). For postoperative prophylactic care, enrofloxacin (50 mg/mL; Bio Pharmachemie Company, Vietnam) was diluted 1:50 in sterile 0.9% NaCl to a final concentration of 1 mg/mL. The diluted solution was administered subcutaneously once daily at a dose of 5 mg/kg, which was within the reported dosage range for veterinary enrofloxacin use (Plumb, 2018). Treatment was continued for five consecutive days following surgery. The five-day administration period was selected as part of the present postoperative management protocol to provide antimicrobial coverage during the early phase of wound healing and was not intended to represent a universally recommended duration. Additionally, meloxicam (Bio Pharmachemie Company, Vietnam) was administered via intraperitoneal injection at a dose of 28.4 µmol/kg every 24 hours for 5 consecutive days following the surgical procedure (Santos et al., 1998).

Statistical analysis

All statistical analyses were performed using GraphPad Prism 9.0 (GraphPad Software, San Diego, CA, USA). Data were expressed as the mean ± standard deviation (SD). A two-way analysis of variance (ANOVA) was conducted to evaluate the effects of suture type (PALF versus Polyglactin 910), observation day (7, 14, 28, and 45 days post-surgery), and their interaction on each clinical parameter (erythema, edema, exudate formation, secondary infection, and hemorrhage). Before ANOVA, the assumption of normality was assessed using the Shapiro-Wilk test, and homogeneity of variances was assessed using Levene's test. When a significant main effect was detected, post hoc comparisons were performed using Tukey's honestly significant difference (HSD) test for multiple comparisons across observation days. Independent t-tests were used to compare suture types at each individual time point. Statistical significance was defined at a p-value less than 5% ($p < 0.05$).

RESULTS

Chemical composition of untreated pineapple leaf fibers

The FTIR spectra of raw PALF exhibited typical absorption bands of lignocellulosic materials (Figure 1). The band at 1,590.5 cm^{-1} represented the C=C aromatic skeletal vibrations of lignin, which constituted a significant part of pineapple leaves. Additionally, a prominent absorption peak at 1,029.33 cm^{-1} was attributed to the C–O and C–O–C stretching vibrations in β-1,4-glycosidic bonds within cellulose and hemicellulose, reflecting the presence of polysaccharide components in the fiber structure. Meanwhile, the absorption band at 2,360.44 cm^{-1} did not represent chemical bonds in cellulose, hemicellulose, or lignin and was likely due to atmospheric CO_2 or background interference. Thus, the major absorption bands in the FTIR spectra confirmed the lignocellulosic nature (cellulose, hemicellulose, and lignin) of the PALF.

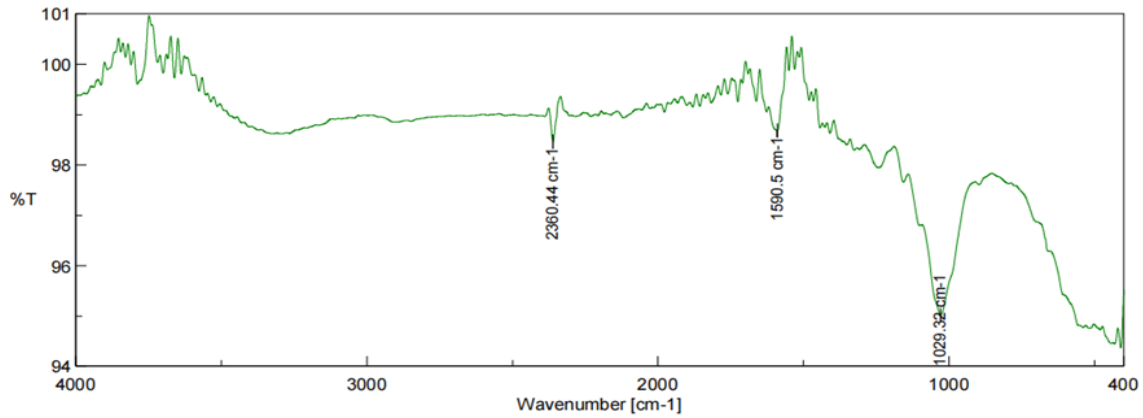

Figure 1. Fourier-transform infrared spectroscopy of untreated pineapple leaf fibers. Fourier-transform infrared spectra of untreated pineapple leaf fibers with major absorption peaks at 1590 cm-1 for C=C stretching of lignin and 1029.33 for C–O and C–O–C glycosidic linkages. The peak at 2360.44 cm-1 represents background CO_2 absorption.

Structure and morphology of treated pineapple leaf fibers

The SEM micrographs revealed that at 1,000x magnification, following 3% NaOH alkaline treatment and TORC/TEMPO-mediated oxidation, the inter-fiber binding components, such as hemicellulose and lignin, were effectively removed. This resulted in a significant amount of treated fiber with bundle defibrillation and a more porous structure, with an average fiber diameter of 53.61 ± 1.89 µm across five measured fibers ($p < 0.05$; Figure 2A). At 2,000x magnification, the fiber surface exhibited prominent longitudinal grooves and a high degree of roughness, characterized by numerous furrows and microstructures extending along the fiber axis. These characteristics enhanced frictional resistance and mechanical interlocking during the fiber spinning process (Figure 2B). The transformation from a smooth surface to a porous, rough structure in treated fibers demonstrated the efficacy of the alkaline treatment and TEMPO-mediated oxidation (chemical treatments) in increasing surface contact area. This structural modification resulted in fundamental biodegradability and tissue-adhesion properties, which were highly critical for its application as a suture material in veterinary surgery. In Figures 2A and 2B, small scattered particles were observed on the fiber surface, possibly attributable to residual debris from the chemical treatments. However, these particles did not form a continuous coating and required further FTIR spectroscopic analysis to identify their chemical nature.

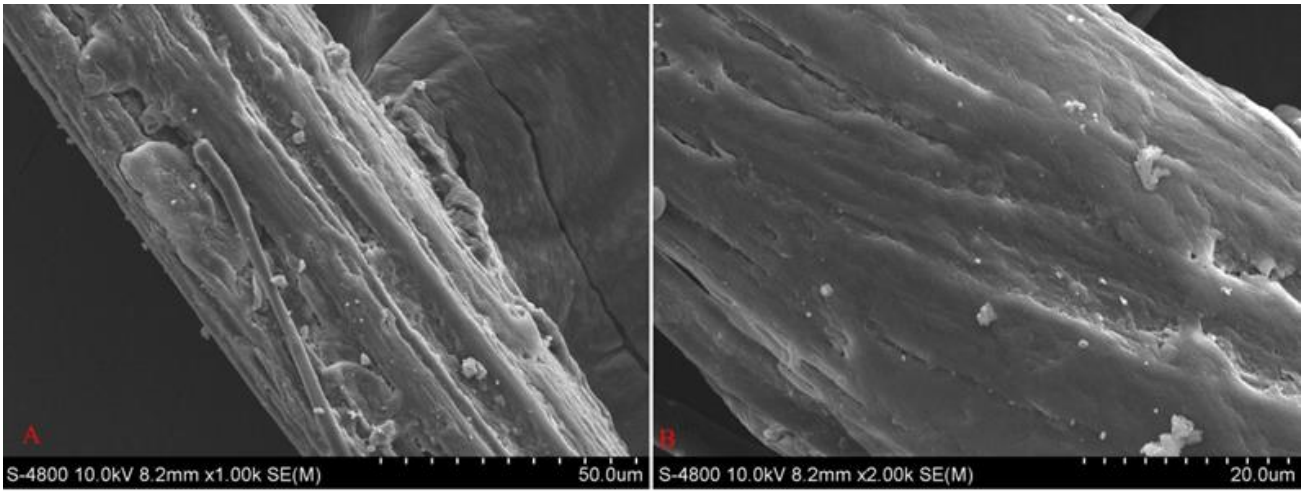

Figure 1. Scanning electron microscope micrographs of pineapple leaf fibers after alkaline treatment and TEMPO-mediated oxidation (TORC). **A**: Fiber structure and bundle defibrillation at 1,000x magnification, **B:** Rough fiber surface and longitudinal grooves at 2,000x magnification

Figure 3 illustrates the FTIR spectra of treated fibers, revealing a broad band in the 3,500-3,200 cm^{-1} range, which corresponds to the -OH stretching of cellulose molecules. Following chemical treatment, the increased intensity of the peak near 3,300 cm^{-1} indicated greater exposure of hydroxyl groups within the polysaccharide backbone of PALF. The peak at 2,915.84 cm^{-1} corresponded to the symmetric C–H stretching vibrations of CH_2 groups, typical of cellulose and hemicellulose. In the spectra of the PALF-treated fibers, only a weak absorption peak at 1,158.53 cm^{-1} was observed, attributed to the arabinose side chains in hemicellulose. The peak at 1,590.5 cm^{-1}, which indicated C=C aromatic skeletal vibrations of lignin, disappeared after treatment. This indicated a significant decrease in intensity compared to the raw

PALF spectrum, in which the lignin-associated peak was observed at 1,590.5 cm^{-1} ($p < 0.05$; Figure 1). This finding confirmed that lignin was partially removed from the fiber structure. The peak at 2,359.96 cm^{-1} was attributed to atmospheric carbon dioxide (CO_2) interference from the environment or equipment, rather than to chemical bonds in the lignocellulosic components. The emergence of a peak at 431.012 cm^{-1} in the 500-150 cm^{-1} range, characteristic of metal-halogen bond vibrations (M-Cl, M-Br, M-F), suggested the potential presence of inorganic salt residues, such as NaCl or NaBr, remaining in the sample after treatment. Furthermore, absorption peaks at 1,630.52 cm^{-1} and 1,314.25 cm^{-1} indicated the asymmetric stretching vibrations of carboxyl groups ($–COO^–$). Consequently, regenerated cellulose produced via TEMPO-mediated oxidation (TORC) yielded a fiber material suitable for sutures, exhibiting both biodegradability and optimal mechanical properties.

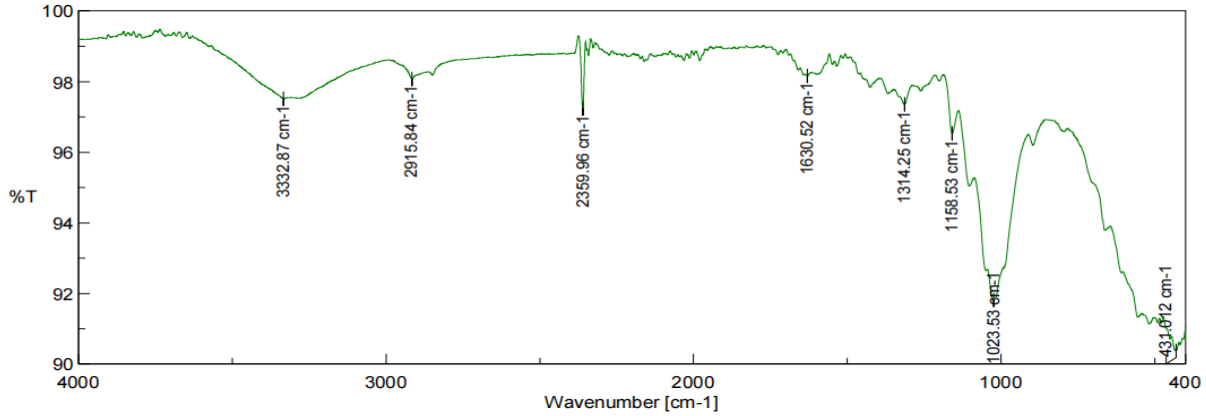

Figure 2. Fourier-transform infrared spectroscopy spectra of pineapple leaf fibers after treatment with alkaline and intermediate oxidation (TEMPO). Fourier-transform infrared spectra of treated pineapple leaf fibers with major absorption peaks at 3500-3200 cm^{-1} for O–H stretching vibrations of cellulose, 2915.84 cm^{-1} for symmetric C–H stretching of CH_2 groups, and 1630.52 cm^{-1} and 1314.25 cm^{-1} for asymmetric stretching of carboxylate groups ($–COO^–$). Additionally, the peaks at 1158.53 cm^{-1} and 431.01 cm^{-1} represent arabinose side chains of hemicellulose and metal–halogen bond vibrations (M–Cl, M–Br, M–F), respectively. The peak at 2359.96 cm^{-1} represents atmospheric CO_2 absorption.

In vitro degradation evaluation of pineapple leaf fiber suture

After two weeks of *in vitro* experiment, the PLAF suture retained its fibrous form; however, the PLAF suture exhibited a significant reduction in tensile strength compared to the original sample of PLAF ($p < 0.05$). By the fourth week, the fiber surface had lost its structural homogeneity, with fibrillation and strand separation observed at multiple sites. The current findings indicated a clear degradation in mechanical properties, with the fiber becoming more brittle, exhibiting decreased elasticity, and being prone to fracturing under minimal mechanical stress. Empirical results indicated that the single-strand suture samples of PALF had a maximum breaking force of about 2.5 ± 0.6 N (approximately 180-330 gf), effectively establishing the mechanical limits and breaking strength of these samples. A high length-to-diameter ratio facilitated the development of an effective fiber network, enabling small-diameter fibers (average diameter of 53.61 ± 1.89 µm) to be transformed into 3/0-grade medical sutures.

Animal bio-assay and *in vivo* analyses of pineapple leaf fiber sutures

Erythema and edema

The present results indicated that observation day significantly affected erythema scores ($F = 18.83$, $p < 0.05$), while suture type did not have a significant main effect ($F = 1.50$, $p > 0.05$; Table 2). There was no significant interaction between suture type and observation day ($F = 0.61$, $p > 0.05$). The current results revealed that scores on days 7 (2.00 ± 0.63) and 14 (1.50 ± 0.55) were significantly higher than those on days 28 (0.67 ± 0.51) and 45 (0; $p < 0.05$), with no significant difference between days 7 and 14 or between days 28 and 45 ($p > 0.05$). Both suture types elicited peak inflammatory responses on day seven post-surgery. Sites sutured with PALF sutures had an erythema score of 2.33 ± 0.58, compared to 1.67 ± 0.58 for those with Polyglactin 910. However, this difference was not statistically significant ($p > 0.05$). Erythema gradually decreased over time, with minimal signs by day 28 (0.67 in both groups) and complete resolution by day 45. Similarly, a significant main effect of observation day was found for edema scores ($F = 11.46$, $p < 0.05$), whereas no significant main effect of suture type ($F = 3.13$) or interaction effect ($F = 1.13$) was observed ($p > 0.05$). The current results indicated that edema scores on day seven (1.83 ± 0.75) were significantly higher than those on days 28 (0.67 ± 0.52) and 45 (0; $p < 0.05$), while day 14 score (1.33 ± 0.82) was not significantly different from any other time point ($p > 0.05$). Edema peaked on day seven, with PALF sutures scoring higher (2.33 ± 0.58) than Polyglactin 910 (1.33 ± 0.58), but the difference was not statistically significant ($p > 0.05$). By day 45, edema had completely resolved in both groups.

Exudation and clinical complications

Exudate formation demonstrated a significant effect based on the observation day ($F = 11.46$, $p < 0.05$), but there was no significant effect of suture type ($F = 1.12$, $p > 0.05$; Table 2). The current findings demonstrated that exudate scores on day seven (1.67 ± 0.81) were significantly higher than those on days 28 and 45 (0; $p < 0.05$), while the day 14 score (0.83 ± 0.75) was not significantly different from any other time point ($p > 0.05$). Exudation was primarily observed within the first 14 days post-surgery. At day seven, PALF sutures exhibited higher exudate scores (2.00 ± 1.00) than Polyglactin 910 (1.33 ± 0.58), although this difference was not statistically significant ($p > 0.05$). From day 28 onward, exudation was absent in both groups.

Secondary infection

Both suture type and observation day significantly affected secondary infection scores ($p < 0.05$), with effects having F values of 6.00 and 5.33, respectively, indicating their individual impact on infection rates. However, the interaction effect was not statistically significant ($F = 2.44$, $p > 0.05$; Table 2). The current results indicated that infection scores on day seven (1.00 ± 0.89) were significantly higher than those on days 28 and 45 (0; $p < 0.05$), while the day 14 score (0.33 ± 0.82) was not significantly different from any other time point ($p > 0.05$). Notably, PALF sutures demonstrated superior performance against secondary infection, with a significantly lower mean infection score (0.08 ± 0.28) than Polyglactin 910 (0.58 ± 0.90) throughout the observation period ($p < 0.05$). Independent t-tests conducted at each time point indicated that the most significant difference occurred on day seven, with PALF sutures having lower infection scores (0.33 ± 0.58) than Polyglactin 910 (1.67 ± 0.58).

Hemorrhage

The observation day had a significant impact on hemorrhage scores ($F = 4.50$, $p < 0.05$). The present results demonstrated that hemorrhage scores on day seven (0.50 ± 0.55) were significantly higher than those on days 14, 28, and 45 (0; $p < 0.05$). In contrast, suture type demonstrated no significant effect ($F = 0.50$), and there were no interaction effects ($F = 0.50$, $p > 0.05$). Hemorrhages were mild and limited to the first seven days after surgery, with complete recovery by day 14 in both groups.

Overall clinical outcomes

From day 28 to day 45, no signs of systemic infection or tissue necrosis were recorded in either group. By day 45 after surgery, all clinical signs of inflammation, such as erythema, edema, exudate, secondary infection, and hemorrhage, had completely resolved in both treatment groups. No wound dehiscence or marginal necrosis was observed in any of the mice.

Table 2. Assessment of clinical parameters for pineapple leaf-derived absorbable sutures and polyglactin 910 sutures at 7, 14, 28, and 45 days post-implantation

Clinical parameters	Suture type (L)	Observation day (N)				Mean (L)
		7	14	28	45	
Erythema	PALF	2.33 ± 0.58	1.67 ± 0.58	0.67 ± 0.58	0	1.67 ± 1.03
	Polyglactin	1.67 ± 0.58	1.33 ± 0.58	0.67 ± 0.58	0	0.92 ± 0.79
Mean (N)		2.00 ± 0.63^{a}	1.50 ± 0.55^{a}	0.67 ± 0.51^{b}	0^{b}	
$F_L = 1.50^{ns}$, $F_N = 18.83^{***}$, $F_{L\times N} = 0.61^{ns}$						
Edema	PALF	2.33 ± 0.58	1.67 ± 1.15	0.67 ± 0.58	0	1.17 ± 1.11
	Polyglactin	1.33 ± 0.58	1.00 ± 0.00	0.67 ± 0.58	0	0.75 ± 0.62
Mean (N)		1.83 ± 0.75^{a}	1.33 ± 0.82^{ab}	0.67 ± 0.52^{bc}	0^{c}	
$F_L = 3.13^{ns}$, $F_N = 11.46^{***}$, $F_{L\times N} = 1.13^{ns}$						
Exudate formation	PALF	2.00 ± 1.00	1.00 ± 1.00	0	0	0.75 ± 1.05
	Polyglactin	1.33 ± 0.58	0.67 ± 0.58	0	0	0.50 ± 0.67
Mean (N)		1.67 ± 0.81^{a}	0.83 ± 0.75^{ab}	0^{b}	0^{b}	
$F_L = 1.12^{ns}$, $F_N = 11.46^{***}$, $F_{L\times N} = 0.46^{ns}$						
Secondary infection	PALF	0.33 ± 0.58	0.67 ± 1.16	0	0	0.08 ± 0.28^{B}
	Polyglactin	1.67 ± 0.58	0	0	0	0.58 ± 0.90^{A}
Mean (N)		1.00 ± 0.89^{a}	0.33 ± 0.82^{ab}	0^{b}	0^{b}	
$F_L = 6.00^{*}$, $F_N = 5.33^{**}$, $F_{L\times N} = 2.44^{ns}$						
Hemorrhage	PALF	0.67 ± 0.58	0	0	0	0.17 ± 0.39
	Polyglactin	0.33 ± 0.58	0	0	0	0.08 ± 0.28
Mean (N)		0.50 ± 0.55^{a}	0^{b}	0^{b}	0^{b}	
$F_L = 0.5^{ns}$, $F_N = 4.5^{*}$, $F_{L\times N} = 0.5^{ns}$						

PALF: Pineapple leaf-derived absorbable sutures, Polyglactin: Polyglactin 910 sutures, L: Suture type factor, N: Observation day factor, F_L: F-value for the main effect of suture type, F_N: F-value for the main effect of observation day, $F_{L\times N}$: F-value for the interaction effect between suture type and observation day, ns: Not significant ($p > 0.05$), *****: $p < 0.05$, ******: $p < 0.01$, *******: $p < 0.001$. Data are expressed as mean ± standard deviation (SD). ^{a,b,c} Mean different superscript letters within the same row indicate statistically significant differences between observation days at $p < 0.05$. $^{A, B}$ Mean different uppercase superscript letters within the same column indicate statistically significant differences between suture types at $p < 0.05$.

DISCUSSION

In the present study, PALF were mechanically decorticated by scraping and subjected to an alkaline treatment (3% NaOH) to solubilize non-cellulosic components, such as lignin and hemicellulose. This process defibrillated clustered bundles and increased surface roughness, which in turn improved the inter-fiber friction during fabrication. These characteristics, referring to the length and strength of cellulose, remain unchanged under mechanical scraping and alkaline treatment (3% NaOH), consistent with the findings of Amornsakchai et al. (2023). The FTIR spectra demonstrated a strong presence of cellulose in PALF. Furthermore, the PALF/PBS material exhibited a flexural strength of 70.7 MPa, a flexural modulus of 2.0 GPa, and a heat deflection temperature of 107.3 °C, which were consistent with the findings of Amornsakchai et al. (2023).

The TEMPO-mediated oxidation system (TORC) successfully converted hydroxyl groups to carboxyl groups (–COO–), which was verified by FTIR absorption peaks at 1630.52 cm^{-1} and 1314.25 cm^{-1}. This TORC technology was similarly utilized by Park et al. (2023) to produce TEMPO-oxidized lignocellulose nanofibrils (TOLCNF). Furthermore, Park et al. (2023) reported that integrating silver nanoparticles was a promising approach to imparting antibacterial properties. Mathew et al. (2024) suggested that these antibacterial effects could be essential in reducing secondary infections observed on day seven in the PALF suture site. The biocompatibility of PALF sutures was comparable to that of the commercial control, Polyglactin 910, with no notable differences observed in erythema or edema responses. *Peristrophe bivalvis* (Magenta) extract was used solely as a natural coloring agent to enhance the visual contrast of sutures against surrounding tissues and blood during surgical observation. This purple color facilitated suture identification and handling rather than serving as an experimental factor. In the present study, there were no significant effects on the degradation behavior or inflammatory response of the PALF suture.

The degradation mechanism of PALF, determined by TEMPO-mediated oxidation, revealed hydrolytic behavior comparable to that of synthetic polymers. Antoniac et al. (2021) reported that in PBS medium (pH 7.2–7.6), fibrillation and fiber separation occurred, leading to a decrease in tensile strength by the fourth week. Antoniac et al. (2021) demonstrated that polyglycolic acid samples and poly lactic-co-glycolic acid entirely lost their load-bearing capacity within 4-6 weeks of immersion due to their highly hydrophilic properties. Because the purified PALF in the present study had a high cellulose content and an optimal crystallinity index, it ensured knot security and biosafety for modern veterinary surgery.

The FTIR spectrum of untreated PALF exhibited characteristic absorption bands indicative of its lignocellulosic nature. The broad absorption band in the 3,200- 3,600 cm^{-1} region corresponded to O–H stretching associated with hydrogen bonding in cellulose, hemicellulose, and lignin, which was consistent with the FTIR characteristics of lignocellulosic fibers reported by Mandal and Chakrabarty (2011). Similarly, the presence of lignin in the untreated PALF was confirmed by the C=C aromatic skeletal band at 1,590.5 cm^{-1}, comparable to the lignin-associated peaks previously observed in natural plant fibers. Furthermore, the dominant absorption peak at 1,029.33 cm^{-1} corresponded to the C–O–C stretch of β-1,4-glycosidic bonds, consistent with the cellulose polysaccharide backbone reported by Kacuráková et al. (2000). These functional groups confirmed that the untreated PALF possessed a typical lignocellulosic structure composed mainly of cellulose, hemicellulose, and lignin. After alkaline treatment and intermediate oxidation (TEMPO), a broad absorption band in the 3,500-3,200 cm^{-1} region appeared in both untreated and treated PALF, consistent with the hydroxyl (-OH) stretching vibrations in the cellulose structure of plant fiber reported by Mandal and Chakrabarty (2011). Although cellulose and hemicellulose both contain similar oxygen-containing functional groups (Yang et al., 2007), the effectiveness of the purification was verified by the disappearance or only a very weak hemicellulose-specific peak at 1,158.53 cm^{-1} (Zhang et al., 2021). The findings reported by Zhang et al. (2021) were consistent with the present study, demonstrating that the chemical treatment successfully removed the majority of the hemicellulose from the fiber structure. Notably, the appearance of peaks at 1,630.52 cm^{-1} and 1,314.25 cm^{-1} corresponded to the stretching vibrations of carboxyl groups ($–COO^-$). These findings aligned with the typical locations of carboxyl groups as reported by Kaya (2025). The formation of carboxyl groups on the surface of regenerated cellulose not only confirmed the effectiveness of the fiber functionalization process but also provided a critical basis for producing suture materials with biodegradability and ideal mechanical properties for biomedical applications.

The surface morphology of the PALF sutures after chemical treatment was crucial to understanding the material's biomechanical performance in surgical use. The presence of deep longitudinal grooves and distinct fibrillation indicated that amorphous binding components, mainly hemicellulose and lignin, have been effectively removed. These morphological changes were consistent with previous studies of Tanpichai and Witayakran (2017) and Gnanasekaran et al. (2021), who reported increased surface roughness and enhanced fiber bundle separation following chemical treatment of PALF. From a veterinary surgical perspective, this PALF surface restructuring offered particularly crucial clinical advantages. First, the highly roughened surface would increase the friction coefficient between the suture loops.

According to Wong and McGrouther (2023), surface roughness was identified as a key factor enhancing knot security compared with smooth synthetic monofilament sutures, thereby decreasing the risk of wound dehiscence due to strong postoperative movement in animals. Second, the presence of microgrooves and a porous structure notably increased the material's specific surface area. Ashworth et al. (2014) demonstrated that material porosity directly influenced fluid diffusion capacity and degradation rate, thereby allowing the infiltration of biological fluids and cellular proteolytic enzymes during *in vivo* degradation. In an *in vivo* environment, these microgrooves and porous structures enabled tissue fluids to permeate quickly and allowed inflammatory cells, such as macrophages and foreign-body giant cells, to infiltrate more easily. Märtson et al. (1999) indicated that the presence of these biological fluids and cellular components led to a gradual, multi-faceted degradation process. This process involved chemical and biological breakdown of the cellulose matrix, accompanied by microstructural fragmentation. Thus, the porous microstructure and improved fluid permeation supported the suture's stable, controlled degradation, meeting the key criteria for an ideal absorbable biomaterial.

Erythema and edema reached their highest levels on day seven, aligning with the acute inflammatory phase. Pathologically, the presence of suture material attracted macrophages and neutrophils to the foreign-body site to clear cellular debris, resulting in vasodilation, serous exudation, and surrounding soft-tissue edema (Fawi et al., 2023). The rapid decline in inflammatory indices from days 7 to 28 correlated with the initiation of fibroblast proliferation and granulation tissue formation as the mucosal barrier gradually closed. By day 45 post-surgery, all inflammatory scores had returned to zero, indicating the normal physiological state of a healthy subject. This baseline score confirmed that the immune system has successfully cleared the foreign material through phagocytosis. Furthermore, the connective tissue at the surgical site has fully recovered and remodeled, with no clinical complications observed. These clinical outcomes of the present study confirmed that PALF sutures and Polyglactin 910 sutures were safe, medical-grade materials with excellent biocompatibility, and followed the same healing process. The absence of major complications, evidenced by the lack of systemic infection or tissue necrosis in all mice, further demonstrated that both materials supported normal wound healing without triggering severe immune rejection. However, in terms of mean values, Polyglactin 910 material consistently demonstrated superiority, with lower scores for edema, erythema, and exudation than PALF sutures, particularly during the first 14 post-operative days. Both PALF sutures and Polyglactin 910 were multifilament materials; this discrepancy in inflammation levels was primarily due to differences in manufacturing technology. Multifilament sutures consist of numerous braided or twisted fibers. This structure created microscopic spaces that act similarly to capillaries, absorbing tissue fluids and potentially harboring bacteria (Katz et al., 1981; Nappi, 2025). The increased exudation in PALF sutures could be due to a looser braided structure, which enhanced capillarization and led to localized accumulation of inflammatory exudate (Nappi, 2025). Moreover, to reduce the surface roughness of multifilament sutures, manufacturers typically apply a surface coating. The fact that Polyglactin 910 elicited less edema and erythema demonstrated that a smoother coating can reduce tissue drag and limit micro-trauma to nearby capillaries during needle penetration (Utami et al., 2025).

Consistent with the findings of Freudenberg et al. (2004), hydrolytic degradation of absorbable sutures can alter the local chemical environment, potentially affecting tissue response and contributing to the peak inflammation observed at day seven in the present study. These findings were further elucidated by the correlation between the crystallinity index and tissue response. According to Guambo et al. (2020), the mechanical performance and biological resistance of natural fibers are highly dependent on their crystalline structure. Guambo et al. (2020) indicated that high-crystallinity fibers, such as sisal (73%), exhibited superior mechanical properties and a higher ability to prevent biofilm formation compared to more porous, low-crystallinity fibers such as coconut fiber (56%). The removal of hemicellulose and lignin from PALF increased its cellulose purity, thereby enhancing its crystallinity index and optimizing tensile strength and resistance to microbial colonization in surgical applications. Pineapple leaf fiber sutures not only reduced tissue reactions but also eliminated the need for post-healing stitch removal, indicating that these materials could serve as durable and biocompatible options.

CONCLUSION

The present study successfully fabricated absorbable veterinary sutures from PALF through alkaline extraction, TEMPO-mediated oxidation, and a 1% chitosan coating. The chemical treatments successfully eliminated non-cellulosic components, resulting in a micro-grooved surface that greatly improved mechanical quality and knot security during suturing. The sutures were sterilized using gamma irradiation at a dosage of 20 kGy to ensure aseptic conditions for surgical applications. *In vitro* degradation assays confirmed the reliable biodegradation profile of the material in a simulated physiological environment over four weeks. *In vivo* biocompatibility assessments in an albino mouse model demonstrated that the PALF sutures effectively supported tissue healing without inducing systemic inflammatory

responses. Notably, the PALF sutures exhibited superior anti-infective properties compared to the Polyglactin 910 control, reflected by significantly lower secondary infection scores (0.08 ± 0.28 versus 0.58 ± 0.90). By day 45 post-operation, all clinical inflammatory parameters, including erythema and edema, had completely resolved. No wound dehiscence, tissue necrosis, or material-related issues were observed at any point during the entire monitoring period. Bio-processed PALF offered a promising, sustainable biomaterial for veterinary surgery, serving as a basis for future improvements. Despite these clinical results, this study acknowledged limitations due to the absence of X-ray diffraction analysis to quantify changes in the fiber's crystallinity index. Moreover, the potential effects of 20 kGy gamma irradiation on the molecular structure and long-term mechanical stability of cellulose fibers remain to be fully elucidated. Extending clinical validation in canines and felines is crucial for veterinary use. Since PALF eliminated the need for suture removal, further surface-coating optimizations could enhance its biostability and performance across diverse conditions.

DECLARATIONS

Acknowledgements

The authors sincerely express their gratitude to the staff, colleagues, and veterinarians at Nong Lam University in Ho Chi Minh City, Vietnam, for their support in completing the present study.

Authors' contributions

Chau Buu Tran and Thuy Thanh Nguyen conceptualized the present study. Thuong Thi Nguyen, Chau Buu Tran, Thuy Thanh Nguyen, and Khiem Gia Mai collected Herb and pineapple leaves. Thuong Thi Nguyen, Chau Buu Tran, Chau Ngoc Thuy Nguyen, and Khiem Gia Mai prepared the materials and designed the study, performed the procedures, and conducted experiments. Thuong Thi Nguyen, Chau Buu Tran, and Chau Ngoc Thuy Nguyen analyzed and interpreted the data generated. Thuong Thi Nguyen, Chau Buu Tran, Chau Ngoc Thuy Nguyen, Khiem Gia Mai, and Thuy Thanh Nguyen critically reviewed the study. Thuong Thi Nguyen supervised the study. All authors revised and approved the final edition of the manuscript.

Availability of data and materials

The authors of this article confirmed that all data supporting the study's findings are available upon reasonable request.

Competing interests

The authors declared no conflicts of interest.

Ethical considerations

This article was written originally without copying from previously published articles or books, submitted only to the present journal, and did not use any AI tools in preparing or writing the manuscript.

Funding

The authors are grateful to Nong Lam University, Ho Chi Minh City, Vietnam, for providing a scientific research grant for the project ID No. CS-SV25-CNTY-01.

REFERENCES

Abu KN, Mohamed AZ, Zainudin ES, Zakaria S, Azman SKZ, and Abdullah HH (2019). Isolation and characterization of macerated cellulose from pineapple leaf. Bioresources, 14(1): 1198-1209. DOI: https://www.doi.org/10.15376/biores.14.1.1198-1209.

Amornsakchai T, Duangsuwan S, Mougin K, and Goh KL (2023). Comparative study of flax and pineapple leaf fiber reinforced poly (butylene succinate): Effect of fiber content on mechanical properties. Polymers, 15(18): 3691. DOI: https://www.doi.org/10.3390/polym15183691

Al-Assaf S, Coqueret X, Dahlan KZHM, Sen M, and Ulanski P (2016). The radiation chemistry of polysaccharides. International Atomic Energy Agency, Vienna, pp. 49-444. Available at: https://www-pub.iaea.org/MTCD/Publications/PDF/P1731_web.pdf

Akter T, Nayeem J, Quadery AH, Razzaq MA, Uddin MT, Bashar MS, and Jahan MS (2020). Microcrystalline cellulose reinforced chitosan coating on kraft paper. Cellulose Chemistry and Technology, 54(1-2): 95-102. DOI: https://www.doi.org/10.35812/cellulosechemtechnol.2020.54.11

Antoniac I, Antoniac A, Gheorghita D, and Gradinaru S (2021). *In vitro* study on biodegradation of absorbable suture Materials used for surgical applications. Materiale Plastice, 58(2): 130-139. DOI: https://www.doi.org/10.37358/MP.21.2.5484

Aouat T, Kaci M, Lopez-Cuesta JM, Devaux J, and Mahlous K (2019). The effect of gamma irradiation on both morphology and properties of neat poly (lactic acid) (PLA), PLA/microcrystalline cellulose (MCC), and PLA/cellulose nanowhiskers (CNW) fibers. Radiation Physics and Chemistry, 16: 14-23. DOI: https://www.doi.org/10.1016/j.polymdegradstab.2018.11.014

Ashworth JC, Best SM, and Cameron RE (2014). Quantitative architectural description of tissue engineering scaffolds. Journal of the Royal Society Interface, 11(100): 20140714. DOI: https://www.doi.org/10.1179/1753555714Y.0000000159.

Araya-Chavarría K, Rojas R, Ramírez-Amador K, Sulbarán-Rangel B, Rojas O, and Esquivel-Alfaro M (2022). Cellulose nanofibers as functional biomaterial from pineapple stubbles via TEMPO oxidation and mechanical process. Waste and Biomass Valorization, 13: 1749-1758. DOI: https://www.doi.org/10.1007/s12649-021-01619-3

Asim M, Abdan K, Jawaid M, Nasir M, Dashtizadeh Z, Ishak M, and Hoque ME (2015). A review on pineapple leaves fibre and its composites. International Journal of Polymer Science, 2015(1): 950567. DOI: https://www.doi.org/10.1155/2015/950567

Association for testing and materials (ASTM) (2002). Standard test method for tensile properties of yarns by the single-strand method, designation: D 2256-02. West Conshohocken, PA, pp. 1-12. Available at: http://file.yizimg.com/175706/2012013011100905.pdf

Beery AK and Zucker I (2011). Sex bias in neuroscience and biomedical research. Neuroscience & Biobehavioral Reviews, 35(3): 565-572. DOI: https://www.doi.org/doi.org/10.1016/j.neubiorev.2010.07.002

Cagle LA, Franzi LM, Epstein SE, Kass PH, Last JA, and Kenyon NJ (2017). Injectable anesthesia for mice: Combined effects of dexmedetomidine, tiletamine-zolazepam, and butorphanol. Anesthesiology Research and Practice, 2017(1): 9161040. DOI: https://www.doi.org/10.1155/2017/9161040

Devi CRV, Ray R, Koduri S, Moharana AK, and Deepak TS (2023). Clinical equivalence of polyglycolic acid suture and polyglactin 910 suture for subcutaneous tissue closure after cesarean delivery: A single-blind randomized study. Medical Devices: Evidence and Research, 16: 27-36. DOI: https://www.doi.org/10.2147/MDER.S385988

Dharanendra YT, Hindi J, Gurumurthy BM, and Muralishwara K (2025). Influence of alkali treatment in enhancing crystallinity and breaking force of pineapple leaf fiber. Scientific Reports, 15: 36081. DOI: https://www.doi.org/10.1038/s41598-025-19991-8

Esquivel AM, Sulbarán RB, Rojas CO, Chen J, Rodríguez QL, Sáenz AG, and Rojas OJ (2025). Processing of pineapple leaf fibers for the production of oxidized micro-/nanofibrillated cellulose. Polymers, 17(19): 2671. DOI: https://www.doi.org/10.3390/polym17192671.

Evitasari RT, Rahayuningsih E, and Mindaryani A (2019). Dyeing of cotton fabric with natural dye from Peristrophe bivalvis extract. AIP Conference Proceedings, 2085(1): 020055. DOI: https://www.doi.org/10.1063/1.5095033

Fawi HMT, Papastergiou P, Khan F, Hart A, and Coleman NP (2023). Use of monofilament sutures and triclosan coating to protect against surgical site infections in spinal surgery: A laboratory-based study. European Journal of Orthopaedic Surgery and Traumatology, 33: 3051-3058. DOI: https://www.doi.org/10.1007/s00590-023-03534-w

Freudenberg S, Rewerk S, Kaess M, Weiss C, Dorn-Beinecke A, and Post S (2004). Biodegradation of absorbable sutures in body fluids and pH buffers. European Surgical Research, 36(6): 376-385. DOI: https://www.doi.org/10.1159/000081648

Götz A, Senz V, Schmidt W, Huling J, Grabow N, and Illner S (2021). General image fiber tool: A concept for automated evaluation of fiber diameters in SEM images. Measurement, 177: 109265. DOI: https://www.doi.org/10.1016/j.measurement.2021.109265

Guambo MPR, Spencer L, Vispo NS, Vizuete K, Debut A, Whitehead DC, Santos-Oliveira R, and Alexis F (2020). Natural cellulose fibers for surgical suture applications. Polymers, 12(12): 3042. DOI: https://www.doi.org/10.3390/polym12123042

Gnanasekaran S, Nordin NIAA, Hamidi M, and Shariffuddin J (2021). Effect of alkaline treatment on the characteristics of pineapple leaves fibre and PALF/PP biocomposite. Journal of Mechanical Engineering and Sciences, 15(4): 8518-8528. DOI: https://www.doi.org/10.15282/jmes.15.4.2021.05.0671

Gupta V (2025). Potential of natural plant-based materials in the development of biocompatible drug-eluting surgical sutures: A review. Biomedical Materials & Devices, 3: 1125-1149. DOI: https://www.doi.org/10.1007/s44174-024-00259-0

Hazarika P, Hazarika D, Kalita B, Gogoi N, Jose S, and Basu G (2018). Development of apparels from silk waste and pineapple leaf fiber. Journal of Natural Fibers, 15(3): 416-424. DOI: https://www.doi.org/10.1080/15440478.2017.1333071

Jain J and Sinhan S (2022). Pineapple leaf fiber polymer composites as a promising tool for sustainable, eco-friendly composite material. Journal of Natural Fibers, 19(15): 10031-10052. DOI: https://www.doi.org/10.1080/15440478.2021.1993478

Kacuráková M, Capek P, Sasinková V, Wellner N, and Ebringerová A (2000). FT-IR study of plant cell wall model compounds: Pectic polysaccharides and hemicelluloses. Carbohydrate Polymers, 43(2): 195-203. DOI: https://www.doi.org/10.1016/S0144-8617(00)00151-X

Kandimalla R, Kalita S, Choudhury B, Devi D, Kalita D, Kalita K, Dash S, and Kotoky J (2016). Fiber from ramie plant (*Boehmeria nivea*): A novel suture biomaterial. Materials Science and Engineering: C, 62: 816-822. DOI: https://www.doi.org/10.1016/j.msec.2016.02.040

Karner L, Drechsler S, Metzger M, Slezak P, Zipperle J, Pinar G, Sterflinger K, Leisch F, Grillari J, Osuchowski M et al. (2020). Contamination of wounds with fecal bacteria in immuno-suppressed mice. Scientific Reports, 10: 11494. DOI: https://www.doi.org/10.1038/s41598-020-68323-5

Katz S, Izhar M, and Mirelman D (1981). Bacterial adherence to surgical sutures. Annals of Surgery, 194(1): 35-41. DOI: https://www.doi.org/10.1097/00000658-198107000-00007

Kaya M (2025). Characterization of TEMPO-oxidized cellulose nanofiber from biowaste and its influence on molecular behavior of fluorescent rhodamine B dye in aqueous suspensions. Journal of Fluorescence, 35(6): 4053-4063. DOI: https://www.doi.org/10.1007/s10895-024-03824-4

Kilkenny C, Browne WJ, Cuthill IC, Emerson M, and Altman DG (2010). Improving bioscience research reporting: The ARRIVE guidelines for reporting animal research. PLoS Biology, 8(6): e1000412. DOI: https://www.doi.org/10.1371/journal.pbio.1000412

Lalhruaitluangi N and Mandal D (2024). Utilization of pineapple leaf: An alternative for paper and textile industries. Journal of Postharvest Technology, 12(3): 1-10. DOI: https://www.doi.org/10.48165/jpht.2024.12.3.01

Liao S, Chen J, and Wang X (2025). An update on pineapple leaf fibers. Journal of Natural Fibers, 22(1): 2509129. DOI: https://www.doi.org/10.1080/15440478.2025.2509129.

Le HP, Dao ND, Huynh TQ, and Tran TTT (2021). Extraction and purification of anthocyanins from *Peristrophe bivalvis* (L.) Merr. leaf (Acanthaceae) using aqueous two-phase systems. Natural Product Research, 37(10): 1-5. DOI: https://www.doi.org/10.1080/14786419.2021.1952203

Lin C, Zeng T, Wang Q, Huang L, Ni Y, Huang F, Ma X, and Cao S (2018). Effects of the conditions of the TEMPO/NaBr/NaClO system on carboxyl groups, degree of polymerization, and yield of the oxidized cellulose. BioResources, 13(3): 5965-5975. DOI: https://www.doi.org/10.15376/biores.13.3.5965-5975

MacArthur Clark JA (2018). 3Rs in research: A contemporary approach to replacement, reduction and refinement. British Journal of Nutrition, 120(S1): S1-S7. DOI: https://www.doi.org/10.1017/S0007114517002227

Mandal A and Chakrabarty D (2011). Isolation of nanocellulose from waste sugarcane bagasse (SCB) and its characterization. Carbohydrate Polymers, 86(3): 1291-1299. DOI: https://www.doi.org/10.1016/j.carbpol.2011.06.030

Märtson M, Viljanto J, Hurme T, Laippala P, and Saukko P (1999). Is cellulose sponge degradable or stable as implantation material? An *in vivo* subcutaneous study in the rat. Biomaterials, 20: 1989-1995. DOI: https://www.doi.org/10.1016/S0142-9612(99)00094-0

Mathew S, Kumar KV, Prabhu A, Shastry RP, and Rajesh KS (2024). Braided silk sutures coated with photoreduced silver nanoparticles for eradicating *Staphylococcus aureus* and *Streptococcus mutans* infections. Journal of Microbiological Methods, 220: 106923. DOI: https://www.doi.org/10.1016/j.mimet.2024.106923

Mayakannan S, Raj JB, Raja VL, and Nagaraj M (2023). Effectiveness of silicon nanoparticles on the mechanical, wear, and physical characteristics of PALF/sisal fiber–based polymer hybrid nanocomposites. Biomass Conversion and Biorefinery, 13: 13291-13305. DOI: https://www.doi.org/10.1007/s13399-023-04654-3

Motaleb KA, Shariful IM, and Hoque MB (2018). Improvement of physicomechanical properties of pineapple leaf fiber reinforced composite. International Journal of Biomaterials, 2018(1): 7384360. DOI: https://www.doi.org/10.1155/2018/7384360

Nair RR, Achari SL, Sharma R, Thomas P, and Rao PR (2023). Essential and fundamental surgical suture techniques for aseptic rodent surgery. ChemRxiv, pp. 1-20. DOI: https://www.doi.org/10.26434/chemrxiv-2023-ch7wt

Nappi F (2025). Suture materials: Conventional and stimulatory-responsive absorbable polymers with biomimetic function. Biomimetics, 10(9): 590. DOI: https://www.doi.org/10.3390/biomimetics10090590

National research council (NRC) (2011). Guide for the care and use of laboratory animals, 8th Edition. National Academies Press., Washington, D.C., pp 105-115. DOI: https://www.doi.org/10.17226/12910

Obernier JA and Baldwin RL (2006). Establishing an appropriate period of acclimatization following transportation of laboratory animals. ILAR Journal, 47(4): 364-369. DOI: https://www.doi.org/10.1093/ilar.47.4.364

Öksüz KE (2024). Bioactive coatings on biopolymer materials: Evaluation of mechanical, physical, thermal, and *in vitro* properties. Journal of the Australian Ceramic Society, 60: 1265-1280. DOI: https://www.doi.org/10.1007/s41779-024-01037-3

Park CW, Bandi R, Dadigala R, Han SY, Kim JK, Kwon GJ, Kim NH, and Lee SH (2023). Wet-spinning of TEMPO-oxidized lignocellulose nanofibrils and functionalization of the filament with Ag nanoparticles. BioResources, 18(1): 505-517. DOI: https://www.doi.org/10.15376/biores.18.1.505-517

Pham TD, Nguyen THD, Tran HD, and Tran TT (2024). Application of satellite images and GIS to assess the site situation and propose solutions for developing pineapple cultivation in U Minh Thuong, Kien Giang, Vietnam. IOP Conference Series: Earth and Environmental Science 1306(1): 012026. DOI: https://www.doi.org/10.1088/1755-1315/1306/1/012026

Pillai CKS and Sharma CP (2010). Absorbable polymeric surgical sutures: Chemistry, production, properties, biodegradability, and performance. Journal of Biomaterials Applications, 25(4): 291-366. DOI: https://www.doi.org/10.1177/0885328210375540

Plumb DC (2018). Plumb's veterinary drug handbook, 9th Edition. Wiley-Blackwell., Ames, Iowa, pp. 588-590. Available at: https://books.google.com.vn/books?id=wshQDwAAQBAJ&printsec=frontcover&hl=vi#v=onepage&q&f=true

Saini R, Chen CW, Patel AK, Saini JK, Dong CD, and Singhania RR (2022). Valorization of pineapple leaves waste for the production of bioethanol. Bioengineering, 9(10): 557. DOI: https://www.doi.org/10.3390/bioengineering9100557

Saini R, Singhania RR, Chen CW, Patel AK, Saini JK, Chauhan AS, and Dong CD (2023). Pineapple leaves waste—A potential feedstock for production of value-added products in biorefinery: Pineapple leaves waste biorefinery. Indian Journal of Experimental Biology, 61(10): 729-738. DOI: https://www.doi.org/10.56042/ijeb.v61i10.1795

Santos A, Vedana E, and De Freitas G (1998). Antinociceptive effect of meloxicam, in neurogenic and inflammatory nociceptive models in mice. Inflammation Research, 47(7): 302-307. DOI: https://www.doi.org/10.1007/s000110050333

Tanpichai S and Witayakran S (2017). All-cellulose composite laminates prepared from pineapple leaf fibers treated with steam explosion and alkaline treatment. Journal of Reinforced Plastics and Composites, 36(16): 1146-1155. DOI: https://www.doi.org/10.1177/0731684417705144

University of Queensland (2021). Standard score sheet for the assessment of wellbeing in rats. University of Queensland, Australia. Available at: https://research-support.uq.edu.au/files/61427/Score%20Sheet_Rats_18_11_2021.pdf

Utami R, Widyarini S, Sutrisno B, Prakoso YA, and Pangaribuan MJA (2025). Effect of *Crescentia cujete* (L.) fruit extract as a thread-coating material for suture implant in rat skin. World Veterinary Journal, 15(2): 274-282. DOI: https://www.doi.org/10.54203/scil.2025.wvj30

Wong YR and McGrouther DA (2023). Biomechanics of surgical knot security: A systematic review. International Journal of Surgery, 109(3): 481-490. DOI: https://www.doi.org/10.1097/JS9.0000000000000298

Yadav VK, Verma N, Kardam SK, and Pullela M (2025). Pineapple leaf fiber in polymer composites: Structure, characterization, and applications. Materials Chemistry and Physics: Sustainability and Energy, 2: 100011. DOI: https://www.doi.org/10.1016/j.macse.2025.100011

Yang H, Yan R, Chen H, Lee DH, and Zheng C (2007). Characteristics of hemicellulose, cellulose and lignin pyrolysis. Fuel, 86(12-13): 1781-1788. DOI: https://www.doi.org/10.1016/j.fuel.2006.12.013

Zhang Y, Wang H, Sun X, Wang Y, and Liu Z (2021). Separation and characterization of biomass components from corn stalk. BioResources, 16(4) : 7205-7222. DOI: https://www.doi.org/10.15376/biores.16.4.7205-7219